technical transactions

No. 2023/009

mechanics

sciendo

Developing the inoculation procedure for high-quality cast iron with flake graphite, intended for large-size casting (bottom or distance plates and counterweights) – produced in Krakodlew Foundry S.A.

Edward Guzik

guz@agh.edu.pl | https://orcid.org/0000-0002-4449-532X

Adrian Świątkowski

adrswi@agh.edu.pl | https://orcid.org/0000-0003-3767-4749

Andrzej Szczęsny

ascn@agh.edu.pl | https://orcid.org/0000-0002-3464-9655

Dariusz Kopyciński

djk@agh.edu.pl | https://orcid.org/0000-0003-1651-2740

Faculty of Foundry Engineering, AGH University of Science and Technology

Piotr Mirek

piotr.mirek@krakodlew.pl

Krzysztof Piotrowski

krzysztof.piotrowski@krakodlew.pl

Krakodlew S.A

Scientific Editor: Jacek Pietraszek, Cracow University of Technology
Technical Editors: Aleksandra Urzędowska, Małgorzata Mazur, Cracow University of Technology Press
Language Verification: Timothy Churcher, Merlin Language Services
Typesetting: Małgorzata Murat-Drożyńska, Cracow University of Technology Press

Received: March 29, 2023
Accepted: September 19, 2023

Copyright: © 2023 Guzik, Świątkowski, Szczęsny, Mirek, Piotrowski, Kopyciński. This is an open access article distributed under the terms of the Creative Commons Attribution License, which permits unrestricted use, distribution, and reproduction in any medium, provided the original author and source are credited.

Data Availability Statement: All relevant data are within the paper and its Supporting Information files.

Funding: The publication was created during the implementation of the RPMP.01.02.01-12-0055 / 18 project at Krakodlew S.A. financed by the Regional Operational Program of the Lesser Poland Voivodeship.

Competing interests: The authors have declared that no competing interests exist.

Citation: Guzik, E., Świątkowski, A., Szczęsny, A., Mirek, P., Piotrowski, K., Kopyciński, D. (2023). Developing the inoculation procedure for high-quality cast iron with flake graphite, intended for large-size casting (bottom or distance plates and counterweights) – produced in Krakodlew Foundry S.A. *Technical Transactions, e2023009*. https://doi.org/10.37705/TechTrans/e2023009

Abstract

This article presents the first part of the research on the production of large-size castings, such as bottom plates and counterweights produced in the Krakodlew S.A. foundry. Castings of this type are not complicated in terms of construction but must meet certain requirements, namely to be able to withstand the effects of high temperature and associated stresses, or to have specific dimensions and weight in the case of counterweights. In both cases, the most common method of forming castings is horizontal moulding. However, this requires a lot of time for machining the finished castings. Forming heavy castings in a vertical orientation, although much more problematic, can mean that the amount of time required for machining may be reduced. The research presents the effect of overheating temperature on the effects of inoculation with the Zircinoc inoculant, in which it was shown that increasing the temperature by fifty degrees increased the amount of eutectic grains by around 11–15%.

Keywords: large-size castings, heavy-weight casting, grey cast iron, inoculation, vertical forming

1. Introduction

Castings of underfloor plates (Fig. 1a) and/or plate weights (Fig. 1b) are classified as large size and heavy casting. Counterweights are dedicated for various types of machinery, mainly for cranes, excavators, drilling machines, forklifts and many others. Counterweights are cleaned up and machined in accordance with specific requirements. They also can be painted to be ready for assembly upon delivery. Plates are cleaned up and depending on the requirements, are associated with such phenomena as: element segregation (Wang, Cheng, Hou, 2020; Wang, Chen, Rong, 2020), graphite flotation, variable proportions of perlite and ferrite, or shrinkage porosity (Benedetti et al., 2017). This also applies to steel castings (Kalandyk et al., 2014; Tęcza & Garbacz-Klempka, 2016; Tęcza & Zapała, 2018) and other groups of materials such as alloy cast iron (Celis et al., 2018; Gilewski et al., 2021; Kopyciński et al., 2016) or castings from the group of large-size structures used, for example, in the power industry.

a) b)



Fig. 1. Examples of counterweight – weight range: up to 30 tons (a) and bottom and distance plates – weight range: up to 80 tons (b) produced in Foundry Krakodlew S.A. (by Krakodlew S.A.)

During casting, there are many problems that make it difficult for foundries to produce castings that meet customer requirements as well as foundry standards and the standardised requirements of EN ISO 8062-3 2007. An important issue in the production of these types of castings is to maintain their dimensions and weight. These moulds can be made horizontally and vertically. In horizontal forming, it is much easier to obtain a similar microstructure in the entire volume of the casting than it is with vertical forming. Furthermore, horizontal forming is easier in terms of the preparation of the mould technology, although it requires a significantly longer machining operation, which significantly increases the cost of producing these types of castings. In the literature, a small number of articles related to large-size and heavy castings and mainly focusing on nodular cast iron (Dobrovska et al., 2009; Foglio et al., 2017; Mourad et al., 2015) and the methods of their production in a vertical arrangement in a casting mould are considered. Usually, foundries prefer to use simpler technology (horizontal system) and longer machining than use more difficult technology (vertical system) with shorter machining. In order to check and develop the technology of producing large-size castings, it is necessary to develop the influence of technological factors, such as the chemical composition of cast iron, the conditions for crystallisation and cooling of castings, the type of moulding mass used, the method of distribution of the casting in the moulding box, which in turn affect the density of the cast iron and its mechanical properties and utility. The literature contains a lot of information about the inoculation of castings with wall thicknesses of up to 2 cm and weights of up to 100 kg. The novel element of this research is exploring the topic of inoculation of cast iron with flake graphite of large-size castings with wall thicknesses of up to 10 cm, which are characterised by a long period of crystallisation and cooling.

2. Research methodology

The tests were planned for a plate with dimensions of 100 x 500 x 500 mm, which was to be made in the Krakodlew foundry. Prior to this, preliminary research was

https://doi.org/10.37705/TechTrans/e2023009

performed at the Department of Cast Alloys and Composites Engineering, Faculty of Foundry Engineering, AGH. For this purpose, a simulation was conducted in the ProCast software and tests of modification of cast iron at different overheating temperatures were performed. The simulation with the ProCAST software was conducted for a plate with dimensions of 100 x 500 x 500 mm for four selected cast iron chemical compositions (Table 1), from which the reference composition was selected. The pouring temperature was 1345°C and the pouring time was 25 seconds.

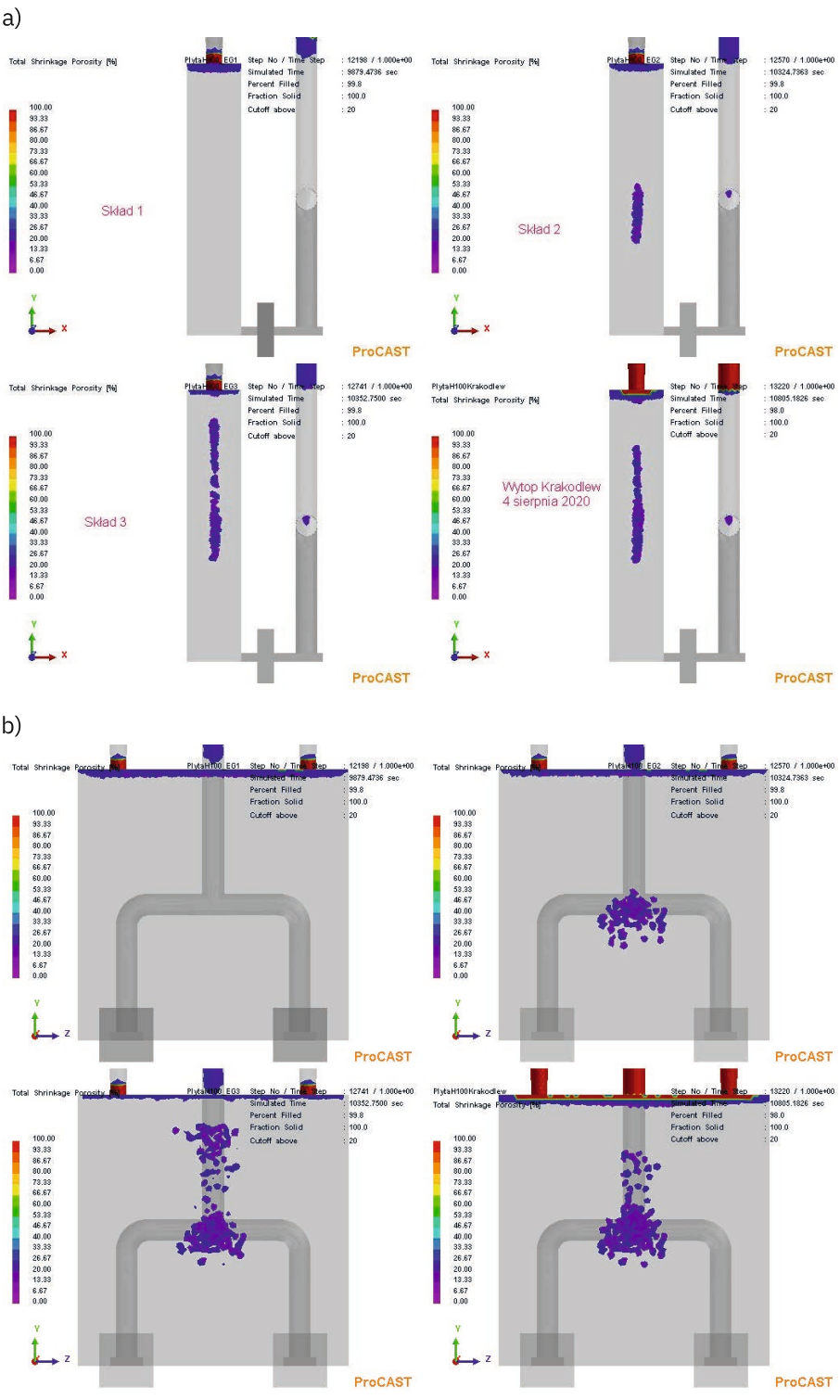


Fig. 2. Simulation results with revealed porosity in the casting (by E. Guzik)

Table 1. Analysed chemical composition of cast iron in the ProCast software

	1	2	3	4
	Chemical composition, % mass			
C	3.40	3.70	3.70	3.90
Si	1.66	1.70	2.00	1.29
Mn	0.60	0.60	0.60	0.68
Cr	0.08	0.08	0.08	0.04
Cu	0.03	0.03	0.03	0.03
Ni	0.02	0.02	0.02	0.02
S	0.04	0.04	0.04	0.018
P	0.10	0.10	0.10	0.069
Carbon saturation degree, Sc	**0.91**	**0.99**	**1.02**	**1.01**
Carbon equivalent, CE	**3.93**	**4.25**	**4.33**	**4.31**

Figures 2a and 2b show the simulation results with the ProCAST software for a 100x500x500mm plate for compositions specified in Table 1.

The chemical composition of the cast iron was selected based on the results of the ProCast simulation. After analysing the simulation results, it was decided that chemical composition no. 1 would be used.

The preliminary research tests were conducted in the Experimental Foundry at the Faculty of Foundry Engineering, AGH, in accordance to the scheme presented in Table 2. The melts were performed in the PIT-30 medium-frequency induction furnace and standard shafts with a diameter of Ø 30 x 270 mm were poured.

Table 2. Preliminary melts

Melt	Metallurgical process	Inoculation process
No. 1	Overheating temperature: 1450C Overheating time: 3 mins	The temperature was lowered to 1400°C. The Zircinoc inoculant was introduced at an amount of 0.35% by mass.
No. 2	Overheating temperature: 1500°C Overheating time: 3 mins	

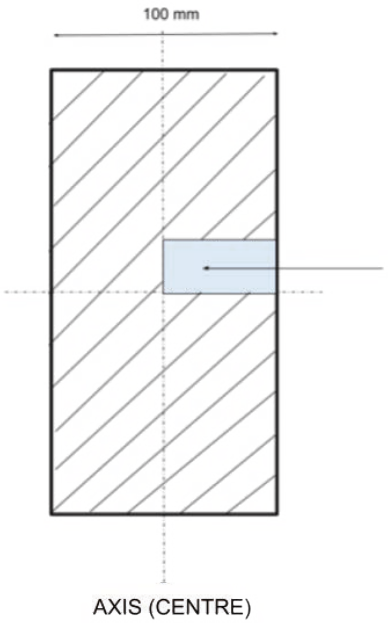


Fig. 3. Location of collecting specimens from the 100-mm-thick plate casting (by A. Świątkowski)

https://doi.org/10.37705/TechTrans/e2023009

Metallographic analysis was performed using a LEICA optical microscope. Quantitative analysis of the test specimens were performed using Leica QWin computer software. In order to determine the size of graphite separations and perlite dispersion and the proportion of perlite in the matrix (Fig. 3) on the cross--section of a 100 mm wall thickness casting, specimens were cut from the centre of plate. Since the heat acceptance in the plate relative to the axis is uniform, samples were taken and subjected to metallographic observation, as indicated in the figure. Specimens were collected from 0, 10, 20, 30, 40 and 50 mm from the centre of the plate casting.

3. Research results

Figures 4 and 5 and table 3 present the results of melt no. 1. Figures 6 and 7 and table 4 present the results of melt no. 2.

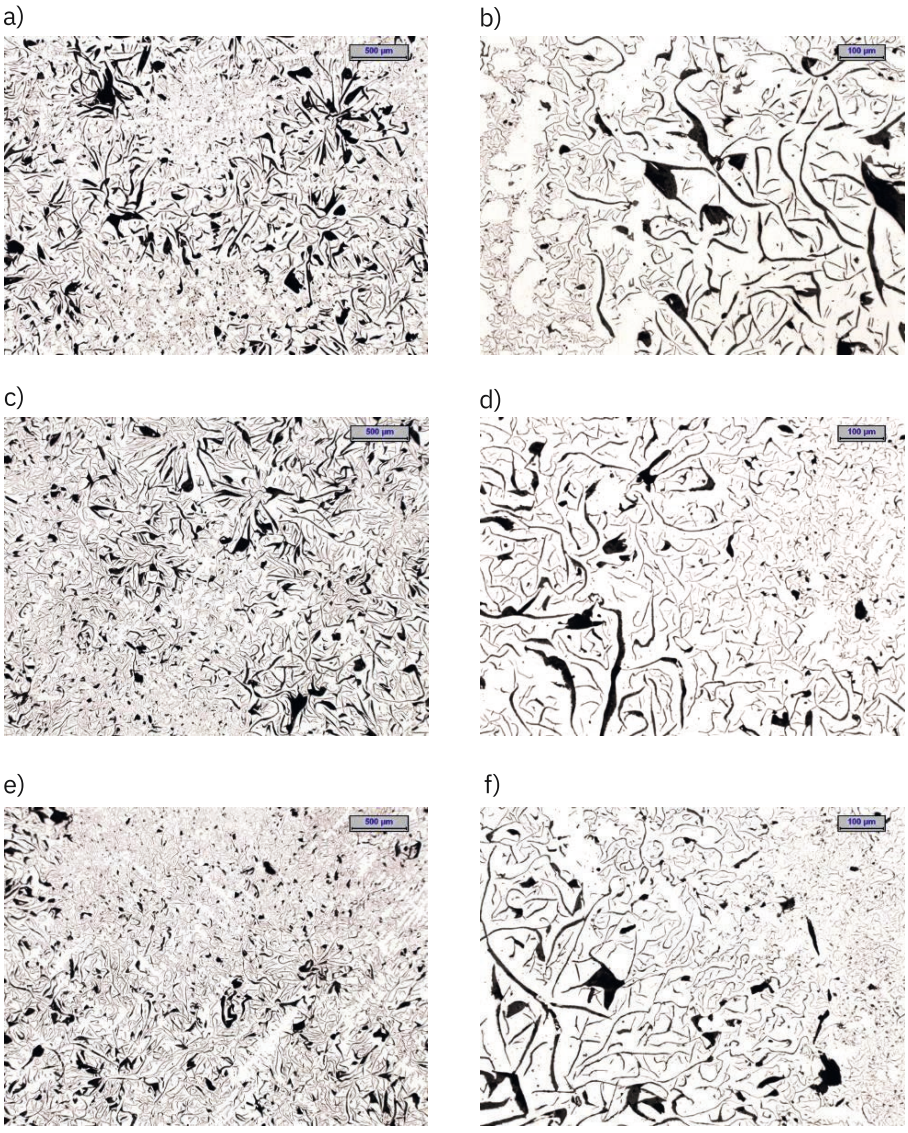


Fig. 4. Melt no. 1. The microstructure of cast iron: a) reference 25x, b) 100x, c) 1 min after inoculation 25x, d) 100x; e) 3 mines after inoculation 25x, f) 100x (by A. Świątkowski)

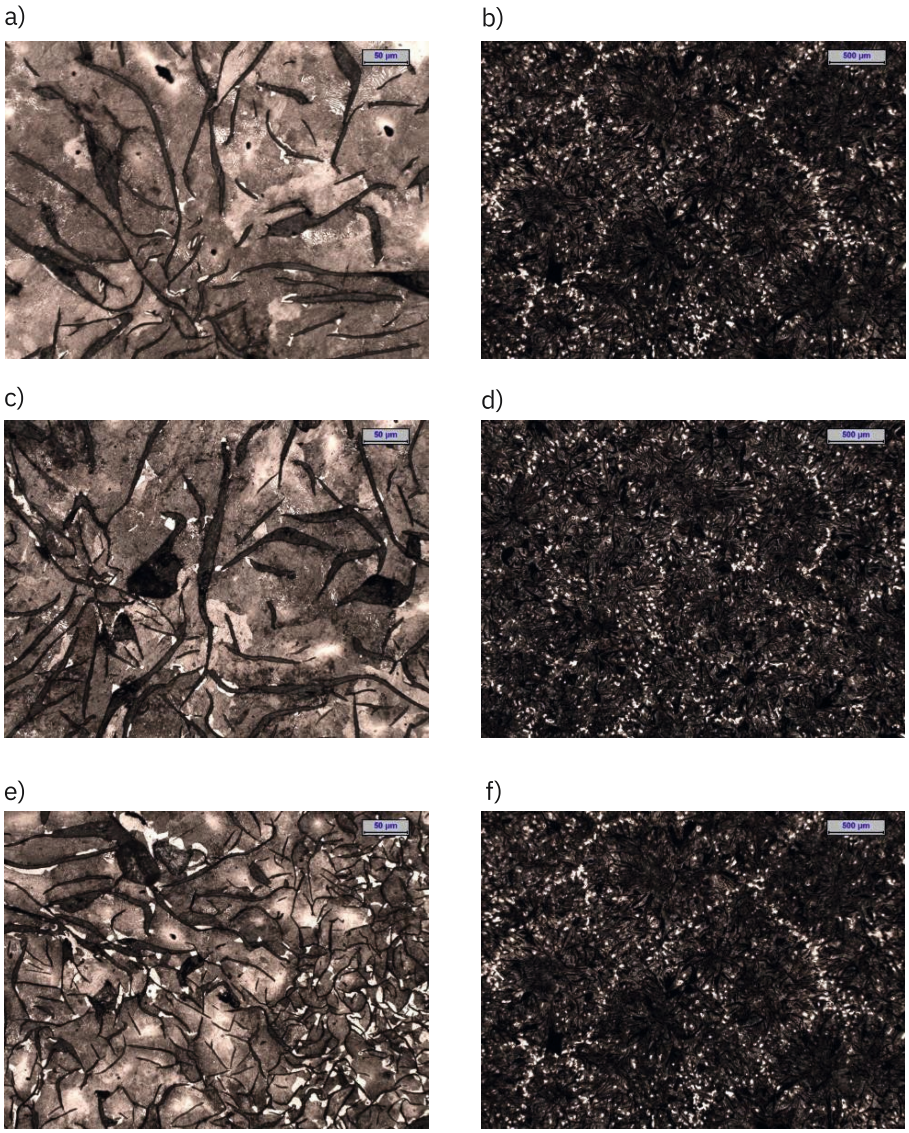


Fig. 5. Melt no. 1. The microstructure of cast iron: a) reference 200x, b) 25x, c) 1 min after inoculation 200x, d) 25x, e) 3 mins after inoculation 100x, f) 25x. Etched Nital – a, c, e; etched Stead – b, d, f (by A. Świątkowski)

https://doi.org/10.37705/TechTrans/e2023009

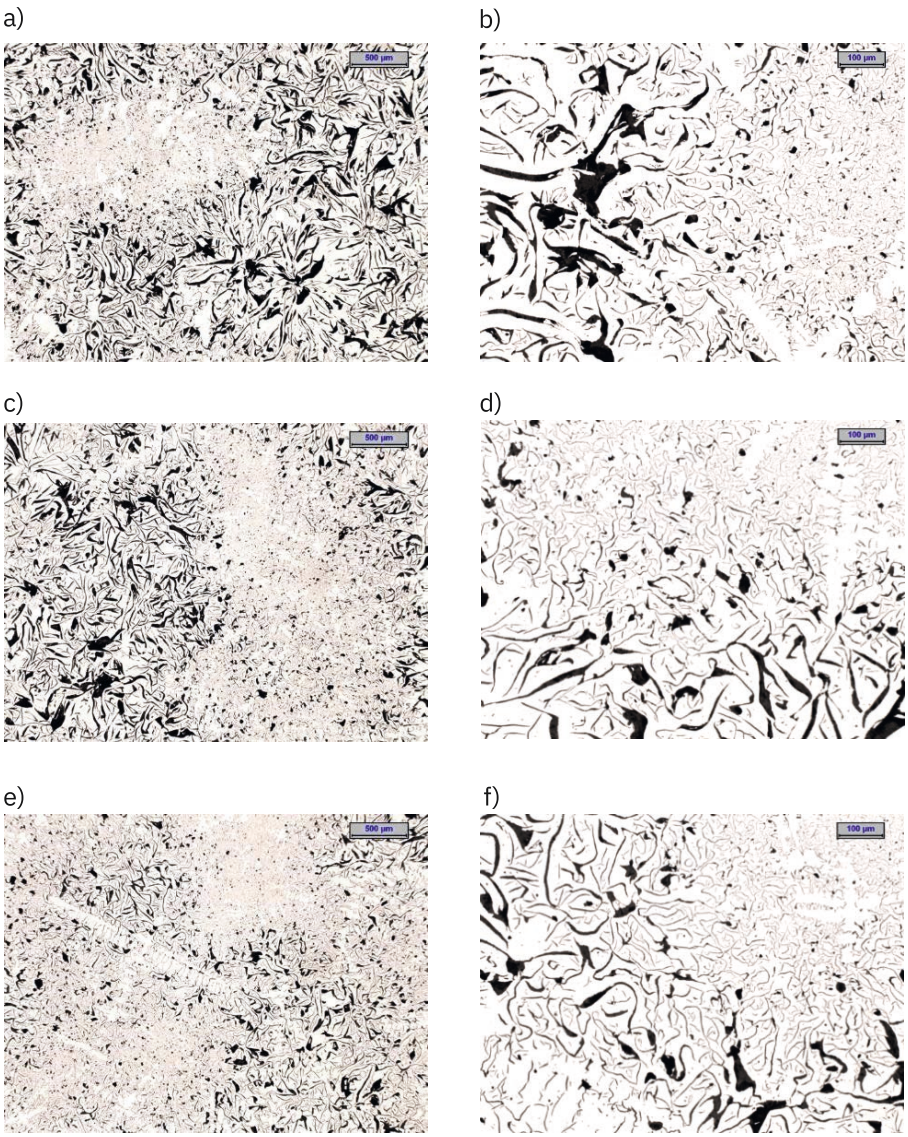


Fig. 6. Melt no. 2. The microstructure of cast iron: a) reference 25x, b) 100x; c) 1 min after inoculation 25x, d) 100x; e) 3 mins after inoculation 25x, f) 100x (by A. Świątkowski)

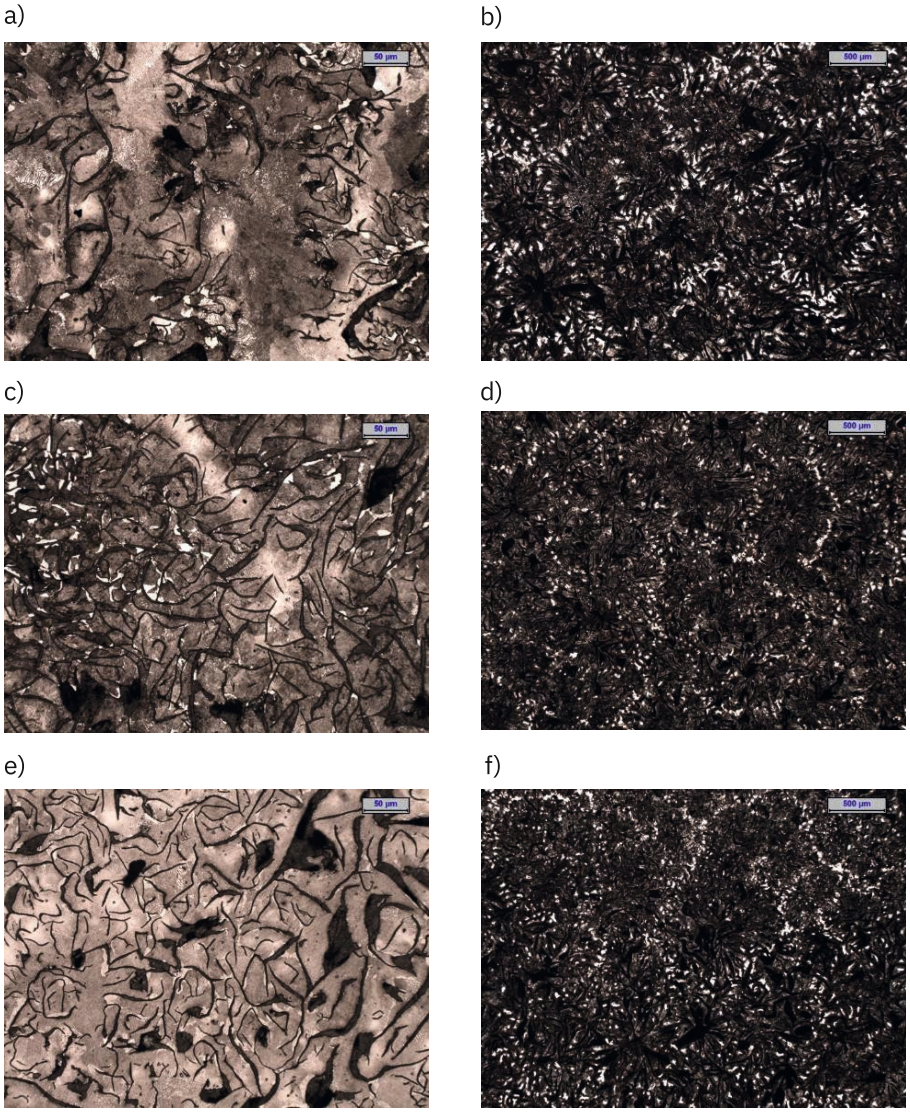
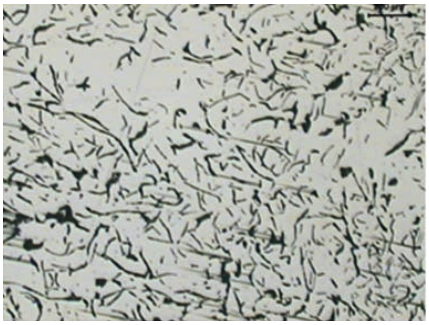


Fig. 7. Melt no. 1. The microstructure of cast iron: a) reference 200x, b) 25x, c) 1 min after inoculation 200x, d) 25x, e) 3 mins after inoculation 100x, f) 25x. Etched Nital – a, c, e; etched Stead – b, d, f (by A. Świątkowski)

https://doi.org/10.37705/TechTrans/e2023009

a)



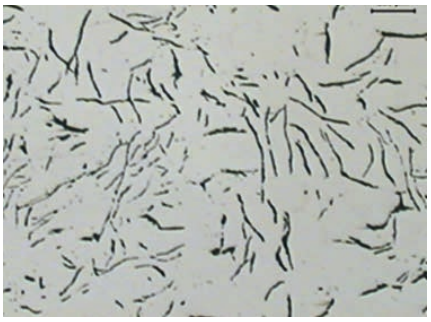
Magnification: 50x
Distance from centre of casting: 10 mm

b)



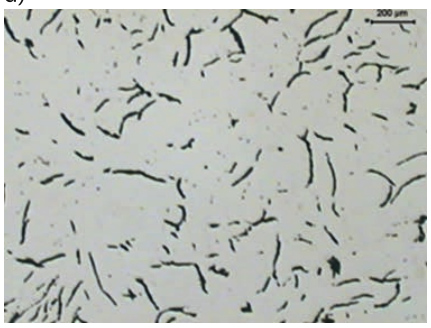
Magnification: 50x
Distance from centre of casting: 20 mm

c)



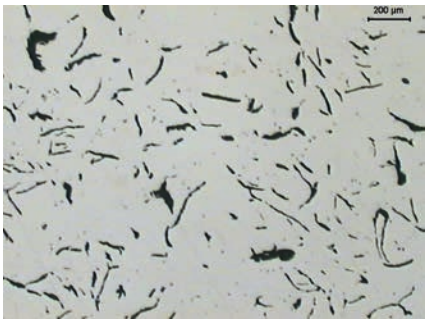
Magnification: 50x
Distance from centre of casting: 30 mm

d)



Magnification: 50x
Distance from centre of casting: 40 mm

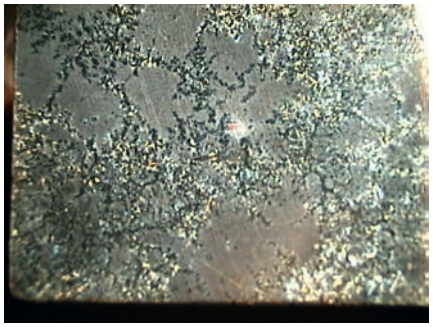
e)



Magnification: 50x
Distance from centre of casting: 50 mm

Fig. 8. Graphite separations of specimens taken from a 100-mm-thick plate (by A. Świątkowski)

a)



Distance from centre of casting: 10 mm

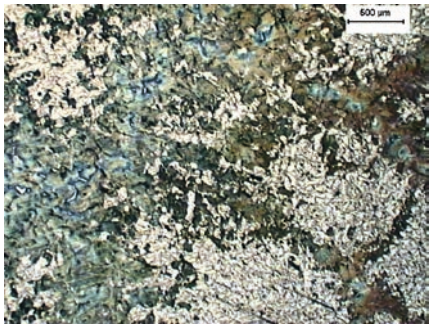
b)



Distance from centre of casting: 50 mm

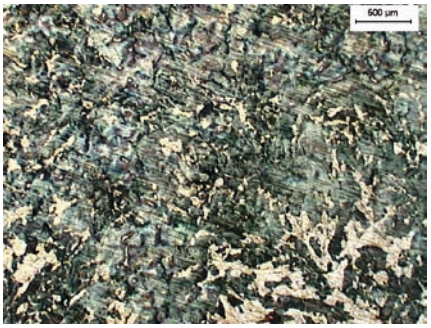
Fig. 9. Eutectic graphite grains of specimens taken from a 100-mm-thick plate – etched with Stead's reagent (by Krakodlew S.A.)

a)



Distance from centre of casting: 0 mm

b)



Distance from centre of casting: 50 mm

Fig. 10. Metal matrix of specimens taken from a 100-mm-thick plate – etched with Nital's reagent (by Krakodlew S.A.)

Table 3. Summary of metallographic results of smelting no. 1. NA – number of grains, % – proportion of graphite, Lmax – maximum size of particles

Melt no. 1							
specimen	NA [cm^{-2}]	type A graphite		type B graphite		type D graphite	
		%	Lmax [µm]	%	Lmax [µm]	%	Lmax [µm]
reference	198	50	431	20	522	30	45
1 min after inoculation	386	75	363	10	508	15	41
3 mins after inoculation	332	50	573	20	611	30	65

Table 4. Summary of metallographic results of smelting no. 2. NA – number of grains, % – proportion of graphite, Lmax – maximum size of particles

Melt no. 2							
specimen	NA [cm^{-2}]	type A graphite		type B graphite		type D graphite	
		%	Lmax [µm]	%	Lmax [µm]	%	Lmax [µm]
reference	190	50	419	30	541	20	52
1 min after inoculation	446	80	462	10	501	10	60
3 mins after inoculation	369	70	449	10	510	20	35

https://doi.org/10.37705/TechTrans/e2023009

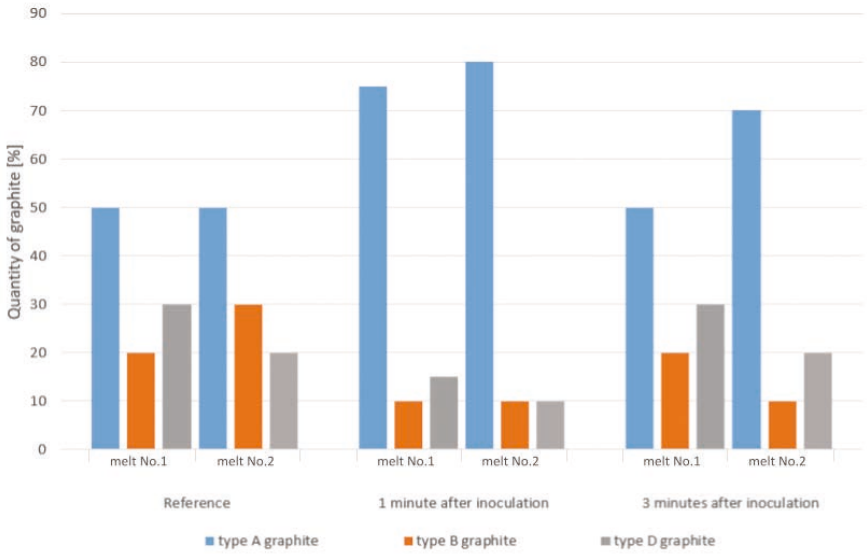


Fig. 11. Metallographic results of smelting no. 1 and no. 2 – proportion of graphite [%] (by A. Świątkowski)

The research showed that superheating the metal to 1500°C increased the proportion of desirable A-type graphite from 50% to 70% and reduced the proportion of undesirable D-type graphite from 30% to 20% after three minutes of inoculation. Increasing the temperature of the metal by 50°C also increased the number of eutectic grains by about 11–15% and contributed to a reduction in the size of graphite particles and an increase in the degree of fragmentation in the microstructure.

Table 5. Summary of metallographic results: size of graphite separations on the cross section of a 100-mm-thick plate

Distance from centre of casting [mm]	Size of graphite separations L [µm]
0	486.5
10	423.4
20	372.5
30	304.8
40	240.9
50	176.8

Table 6. Summary of metallographic results: The proportion of perlite in the matrix on the cross section of a 100-mm-thick plate

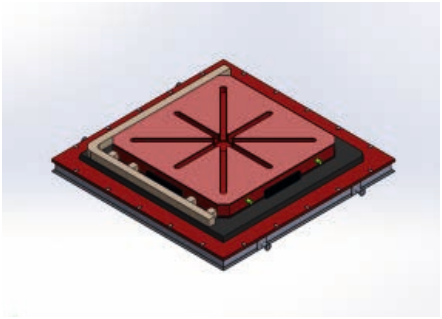
Distance from centre of casting [mm]	The proportion of perlite in the matrix [%]	Determination of the proportion of perlite
0 – centre of the plate	45	P45
25	78	P70
30	82	P85
40	92	P92
50	95	P96

Table 7. Summary of metallographic results: Perlite dispersion on the cross section of a 100-mm-thick plate

Distance from centre of casting [mm]	Perlite dispersion [µm]	Determination of perlite dispersion
0 – centre of the plate	1.61	Pd 1.4
0.7	1.59	Pd 1.4
25	0.68	Pd 0.5
30	0.54	Pd 0.5
40	0.5	Pd 0.5
50	0.46	Pd 0.5

4. Practical application of laboratory research results in industrial research

Laboratory research was replicated in industrial research, in which the pattern was a 2730 x 2730 mm slab with a chills system.



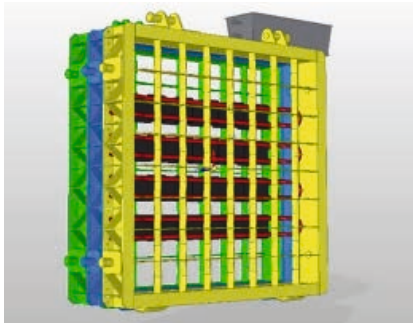
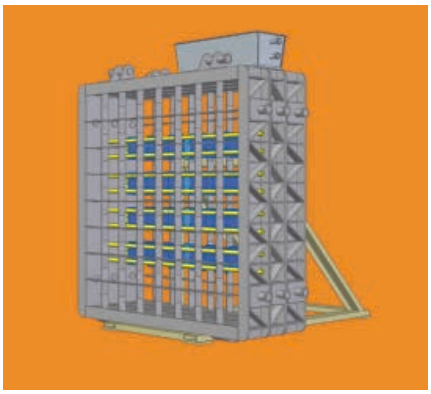


Fig. 12. Plate pattern with dimensions of 2730 x 2730 mm (by Krakodlew S.A.)

Fig. 13. Visualisation of the moulding box with a chills system and moulding accessories (by Krakodlew S.A.)



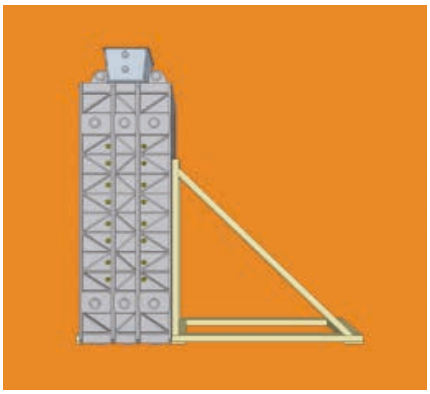


Fig. 14. Layout of the water mist cooling system and chills (by Krakodlew S.A.)

Fig. 15. Place of pouring the mould cavity (by Krakodlew S.A.)

The use of chills at the appropriate locations accelerates the solidification of the casting and results in directed crystallisation. In the case of large-size plate castings (cast in the vertical position), this is particularly important because of the natural occurrence of overheating of the casting in the central part of the casting. Overheating of the casting is associated with overgrowth of crystallisation particles. To prevent this, the Krakodlew S.A. foundry uses chills and water mist cooling.

The mould cooling process begins when the air temperature at the outlet of the cooling system reaches approximately 100°C. This is a required condition for safety reasons. This temperature is checked using a thermal imaging camera (Fig. 16) and thermocouples placed in the cooling system. The water mist in the

https://doi.org/10.37705/TechTrans/e2023009

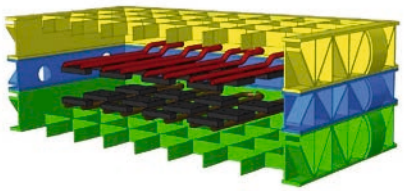


Fig. 16. Distribution of the chills in the moulding box (by Krakodlew S.A.)

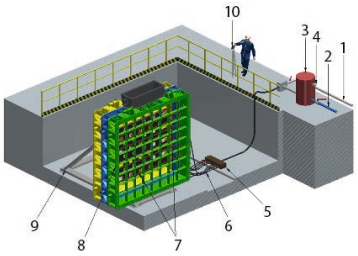


Fig. 17. Station for pouring liquid metal into a mould cavity in a vertical system with a water mist cooling system: 1 – air flow, 2 – water flow, 3 – water mist container, 4 – manometer, 5 – manifold, 6 – pipes connecting the manifold with each segment of the cooling system separately, 7 – chills, 8 – moulding box, 9 – stand for vertical system, 10 – thermal imaging camera (by Krakodlew S.A.)

cooling system is transformed into steam. Steam improves cooling performance and is a safer cooling system than water cooling.

The cooling time is the result of a numerical simulation. This means that each new application of the active chills system requires a new numerical simulation that determines the required cooling velocity and the cooling time needed to achieve optimum results.

5. Conclusions

By analysing the presented research results, the following conclusions can be drawn:

- The results of experimental tests show that the superheating temperature of the metal at 1500°C for three minutes gives much better results in terms of graphite homogeneity compared to the superheat temperature of 1450°C. Such overheating of the metal contributes to the physicochemical state of the liquid alloy, which ensures a more favourable microstructure of the particles of graphite flakes, especially its proper distribution and size.
- The influence of the time from the introduction of the inoculant to the liquid alloy on the shaping of graphite in cast iron was also analysed (disappearance of the modification effect). It was found that the optimal duration of the inoculant reaction (Zircinoc) in molten metal is one minute.
- The size of the separations of graphite and the pearlite dispersion decreases and the proportion of perlite in the matrix increases when the distance from the centre of the plate becomes greater.

References

Benedetti, M., Torresani, E., Fontanari, V., & Lusuardi, D. (2017). Fatigue and Fracture Resistance of Heavy-Section Ferritic Ductile Cast Iron. *Metals*, *7*(3), 88. https://doi.org/10.3390/met7030088

Celis, M., Domengès, B., Hug, E., & Lacaze, J. (2018). Analysis of Nuclei in a Heavy-Section Nodular Iron Casting. *Materials Science Forum*, *925*, 173–180. https://doi.org/10.4028/www.scientific.net/MSF.925.173

Dobrovska, J., Kavicka, F., Stransky, K., Sekanina, B., Stetina, J., Barlat, F., Moon, Y.H., & Lee, M.G. (2009). Numerical Optimization of the Method of Cooling of a Massive Casting of Ductile Cast-Iron. *Materials and Technology*, *43*, 73–78. https://doi.org/10.1063/1.3457606

Foglio, E., Gelfi, M., Pola, A., & Lusuardi, D. (2017). Effect of Shrinkage Porosity and Degenerated Graphite on Fatigue Crack Initiation in Ductile Cast Iron. *Key Engineering Materials*, *754*, 95–98. https://doi.org/10.4028/www.scientific.net/KEM.754.95

Gilewski, R., Kopyciński, D., Guzik, E., & Szczęsny, A. (2021). An Evaluation of the Microstructure of High-Aluminum Cast Iron in Terms of the Replacement of Aluminum Carbide with Titanium Carbide or Tungsten Carbide. *Applied Sciences*, *11*(20), 9527. https://doi.org/10.3390/app11209527

Kalandyk, B., Zapała, R., Sobula, S., Górny, M., & Boroń, Ł. (2014). Characteristics of low nickel ferritic-austenitic corrosion resistant cast steel. *Metalurgija/ Metallurgy*, *53*(4), 613–616.

Kopyciński, D., Siekaniec, D., Szczęsny, A., Sokolnicki, M., & Nowak, A. (2016). The Althoff-Radtke test adapter for high chromium cast iron. *Archives of Foundry Engineering*, *26*(4), 74–77.

Mourad, M.M., El-Hadad, S., Ibrahim, M., & Nofal, A. (2015). Effect of Processing Parameters on the Mechanical Properties of Heavy Section Ductile Iron. *Journal of Metallurgy*, 1–11. https://doi.org/10.1155/2015/931535

Tęcza, G., & Garbacz-Klempka, A. (2016). Microstructure of Cast High--Manganese Steel Containing Titanium. *Archives of Foundry Engineering*, *16*(4), 163–168. https://doi.org/10.1515/afe-2016-0103

Tęcza, G., & Zapała, R. (2018). Changes in impact strength and abrasive wear resistance of cast high manganese steel due to the formation of primary titanium carbides. *Archives of Foundry Engineering*, *18*(1), 119–122. https://doi.org/10.24425/118823

Wang, Q., Cheng, G., & Hou, Y. (2020). Effect of Titanium Addition on As-Cast Structure and High-Temperature Tensile Property of 20Cr-8Ni Stainless Steel for Heavy Castings. *Metals*, *10*, 4–15. https://doi.org/10.1016/j.msea.2006.09.001

Wang, Q, Chen, S., & Rong, L. (2020). δ-Ferrite Formation and Its Effect on the Mechanical Properties of Heavy-Section AISI 316 Stainless Steel Casting. *Metallurgical and Materials Transactions*, *51*(6), 2998–3008. https://doi.org/10.1007/s11661-020-05717-0